



MYCOPLASMA CONTROL

Stop burying your head in the sand.

Your cells could be contaminated with mycoplasma.



This information is current as of June 25, 2014.

CD8 Locus Nuclear Dynamics during Thymocyte Development

Eleni Ktistaki, Anna Garefalaki, Adam Williams, Simon R. Andrews, Donald M. Bell, Katie E. Foster, Charalampos G. Spilianakis, Richard A. Flavell, Nadezda Kosyakova, Vladimir Trifonov, Thomas Liehr and Dimitris Kioussis

J Immunol 2010; 184:5686-5695; Prepublished online 19 April 2010;
doi: 10.4049/jimmunol.1000170
<http://www.jimmunol.org/content/184/10/5686>

Supplementary Material <http://www.jimmunol.org/content/suppl/2010/04/19/jimmunol.1000170.DC1.html>

References This article **cites 74 articles**, 27 of which you can access for free at:
<http://www.jimmunol.org/content/184/10/5686.full#ref-list-1>

Subscriptions Information about subscribing to *The Journal of Immunology* is online at:
<http://jimmunol.org/subscriptions>

Permissions Submit copyright permission requests at:
<http://www.aai.org/ji/copyright.html>

Email Alerts Receive free email-alerts when new articles cite this article. Sign up at:
<http://jimmunol.org/cgi/alerts/etoc>

The Journal of Immunology is published twice each month by
The American Association of Immunologists, Inc.,
9650 Rockville Pike, Bethesda, MD 20814-3994.
Copyright © 2010 by The American Association of
Immunologists, Inc. All rights reserved.
Print ISSN: 0022-1767 Online ISSN: 1550-6606.



CD8 Locus Nuclear Dynamics during Thymocyte Development

Eleni Ktistaki,^{*1} Anna Garefalaki,^{*1} Adam Williams,^{*†} Simon R. Andrews,[‡]
 Donald M. Bell,^{*} Katie E. Foster,^{*2} Charalampos G. Spilianakis,^{†,3} Richard A. Flavell,[†]
 Nadezda Kosyakova,[§] Vladmir Trifonov,[§] Thomas Liehr,[§] and Dimitris Kioussis^{*}

Nuclear architecture and chromatin reorganization have recently been shown to orchestrate gene expression and act as key players in developmental pathways. To investigate how regulatory elements in the mouse CD8 gene locus are arranged in space and in relation to each other, three-dimensional fluorescence in situ hybridization and chromosome conformation capture techniques were employed to monitor the repositioning of the locus in relation to its subchromosomal territory and to identify long-range interactions between the different elements during development. Our data demonstrate that CD8 gene expression in murine lymphocytes is accompanied by the relocation of the locus outside its subchromosomal territory. Similar observations in the CD4 locus point to a rather general phenomenon during T cell development. Furthermore, we show that this relocation of the CD8 gene locus is associated with a clustering of regulatory elements forming a tight active chromatin hub in CD8-expressing cells. In contrast, in nonexpressing cells, the gene remains close to the main body of its chromosomal domain and the regulatory elements appear not to interact with each other. *The Journal of Immunology*, 2010, 184: 5686–5695.

Although epigenetic studies examining histone modifications and chromatin remodeling originally gave contradictory and controversial results, recently a more educated view on how the genome is organized in the nucleus and how genes respond to environmental signals to initiate and establish a transcriptional program has evolved. A number of histone modifications can be used as markers of active transcription (3meK4H3, 3meK36H3, AcH3, AcH4) and a number of chromatin-associated proteins (HP1a, Suv39H) and histone modifications (3meK9H3, 3meK27H3) as hallmarks for silent chromatin. In addition, nuclear architecture has emerged as a key player in creating the conditions for gene activation or silencing.

A prevalent model of nuclear architecture proposes that, with some exceptions, transcribing or permissive euchromatin is located toward the center of the nucleus, whereas the silent heterochromatin lies near the nuclear periphery. Recently, powerful tools, such

as three-dimensional (3D) fluorescence in situ hybridization (FISH) and chromosome conformation capture (3C), have helped toward a better understanding of the functional organization of the genome in lymphocytes and other cell types (1–4) and of how the transcriptional activity could be correlated to a preferential positioning of a gene within the nucleoplasm. Thus, it has been shown that CD4 and CD8 coreceptor genes associate with heterochromatin when silenced during T cell development (5–7).

As transcription and RNA editing factors and RNA pol II are in limiting numbers in the nucleus, their accumulation in the nucleoplasmic “transcription factories” (TFs) (8) provided a mechanism by which the cell could coordinate expression. As TFs are outnumbered by active genes in the cell nucleus, they are thought to be shared by several genes located on the same or different chromosomes.

In interphase, chromosomes occupy “chromosome territories” (CTs) that have a nonrandom organization and distribution within the nucleus (3, 9, 10). Gene density (11–15), guanine-cytosine content (16–18), size of the CTs, and the presence of regulatory sequences, such as locus control regions (LCRs) (19–21) and transcriptional activity (22, 23), all seem to orchestrate the relocation of genes, with active genes or those poised for transcription preferentially found on large chromatin loops that extend several microns away from the CT, increasing their chances for association with TF (24–26). Nevertheless, a number of studies have now reported the presence of active TFs inside the CTs (27).

It is still unclear what controls the generation of these loops or their movements. The interaction of transcription factors (28–30) and regulatory elements that can act at large genomic distances from their target genes may direct and stabilize the formation of the loops. The ability to detect long-range interactions between genomic elements has been facilitated by the development of 3C (31) and other related methods (circular chromosome conformation capture and carbon-copy chromosome conformation capture) (32–35), which are used to detect the physical associations among LCRs, enhancers, and promoters with single (36–42) or multiple genomic loci (43, 44), both in *cis* and in *trans* chromosomal sites. The 3D clustering of regulatory elements and genes has been named active chromatin hub (ACH) (41).

The different stages of thymocyte development can be followed by the expression of the cell-surface coreceptors CD4 and CD8.

^{*}Division of Molecular Immunology, Medical Research Council, National Institute for Medical Research, London; [†]Bioinformatics Group, The Babraham Institute, Cambridge, United Kingdom; [‡]Section of Immunobiology, Yale University School of Medicine, New Haven, CT 06520; and [§]Jena University Hospital, Institute of Human Genetics and Anthropology, Jena, Germany

¹E.K. and A.G. contributed equally to this work.

²Current address: Haematopoietic Stem Cell Laboratory, Cancer Research UK, London Research Institute, London, United Kingdom.

³Current address: Institute of Molecular Biology and Biotechnology, Foundation for Research and Technology, Hellas, Crete, Greece.

Received for publication January 19, 2010. Accepted for publication March 16, 2010.

This work was supported by the Medical Research Council United Kingdom and a European Union Grant (Molecular Imaging, IP503259).

Address correspondence and reprint requests to Dr. Dimitris Kioussis, National Institute for Medical Research, The Ridgeway, Mill Hill, London NW7 1AA, United Kingdom. E-mail address: dkiouss@nimr.mrc.ac.uk

The online version of this article contains supplemental material.

Abbreviations used in this paper: 3C, chromosome conformation capture; 3D, three-dimensional; ACH, active chromatin hub; AV, average; CT, chromosome territory; DN, double-negative; DOP-PCR, degenerated oligonucleotide-primed PCR; DP, double-positive; FISH, fluorescence in situ hybridization; LCR, locus control region; N, number of events; RT, room temperature; sCT, subchromosomal territory; SP, single-positive; TF, transcription factory.

Copyright © 2010 by The American Association of Immunologists, Inc. 0022-1767/10/\$16.00

Thus, early cells are negative for CD4 and CD8 double-negative (DN), subsequently they upregulate both coreceptors to become CD4⁺CD8⁺ double-positive (DP). Further maturation and selection lead to downregulation of either CD4 or CD8, resulting in CD8 single-positive (SP) (CD4⁻CD8⁺) or CD4 SP (CD4⁺CD8⁻) cells, which migrate out of the thymus to populate peripheral lymphoid organs (45).

A number of studies have elucidated the regulation of expression of the two coreceptors (reviewed in Ref. 46). The murine CD8 cell-surface glycoprotein is expressed predominately as a disulphide-bonded heterodimeric molecule composed of an α - and a β -chain (47–49) on thymus derived T cells, whereas other T cells express mainly CD8 α homodimers (50). The two chains (CD8 α /Lyt-2 and CD8 β /Lyt-3) are encoded by two distantly related but closely linked genes, CD8 α and CD8 β , located on chromosome 6 in the mouse, separated by 36 kb, and organized in the same transcriptional orientation (51). Four hypersensitive site clusters (CI–CIV) have been identified in the CD8 locus (52). Studies with transgenic and knockout mice (53–58) revealed a complex regulatory network involving the developmental stage-, subset-, and lineage-specific cooperation of *cis*-regulatory elements in the CD8 locus for the proper expression of CD8 α and CD8 β genes during T cell development.

To gain an insight into how these regulatory elements are arranged in space and in relation to each other, 3D FISH and 3C techniques were employed to monitor the repositioning of the locus in relation to its CT and to identify long-range interactions between the different clusters at different developmental stages.

Materials and Methods

Bacs and cosmids

The CD8 α cosmid was cosCD8 α -1 (52), and the CD4 bac was RP24-545G7.

Staining and sorting of the cells

For the analysis of thymocytes at different developmental stages, thymic cells were isolated from 4–6-wk-old C57BL/6 female mice, and the cells were stained with anti-CD4 and anti-CD8 and were then run on a sorter to a purity of $\geq 90\%$. For the CD4⁻CD8⁻DN population, cells were first depleted of CD4 SP and then stained with anti-CD4 and anti-CD8 as well as a mix of Abs against populations that we wanted to exclude, such as CD11c/Mac1 (macrophages), CD19 (B cells), NK1.1 (NK cells), and Ter119 (erythrocytes). For the studies in the spleen, splenocytes were isolated from 6-wk-old C57BL/6 female mice and stained with anti-TCR, CD4, CD8, and B220 (CD45R). The Abs used for the staining of the cells are listed below. All the Abs were from eBioscience (San Diego, CA) unless otherwise stated. CD4-APC (Caltag Laboratories, Burlingame, CA), CD8 α -FITC (Santa Cruz Biotechnology, Santa Cruz, CA), CD11b-PE, CD19-PE, NK1.1-PE, Ter119-PE, TCR β -PE, and CD45R-FITC (Caltag Laboratories). For the depletion of CD4 SP we used the Histopaque-1119 (Sigma-Aldrich, St. Louis, MO). The different cell populations were sorted on a Cytomation MoFlo High Speed Cell Sorter (Dako, Carpinteria, CA). For the 3C experiments, thymi and spleens of 15 \times C57BL/6 6-wk-old female mice were dissected out and used to make single-cell suspensions. Thymocytes were stained with CD8 α -APC and CD4-PE. Splenocytes were stained with CD45R-FITC (Caltag Laboratories), CD8 α -APC, and CD4-PE.

All experiments were performed in accordance with the guidelines and regulations of the Home Office U.K. and the Ethics Review Panel of the Medical Research Council.

Preparation of the slides

Cells, at a concentration of 3×10^6 /ml, were let to adhere to polylysine pre-coated glass slides for 20 min at room temperature (RT) and then incubated briefly in a hypotonic solution, 0.3 \times PBS, for exactly 1 min to avoid the shrinkage in the following step. They were then fixed in 4% paraformaldehyde in 0.3 \times PBS and permeabilized in 0.05% Triton X-100 in PBS for 10 min at RT. The slides were then transferred to a 20% glycerol solution in 1 \times PBS for overnight incubation prior to three cycles of freezing (liquid nitrogen) and thawing (RT). Between the cycles, the slides were briefly incubated in the glycerol solution. Samples were deproteinized with incubation in 0.1 N HCl for 8 min following, after extensive washing in 1 \times PBS, by incubation in a pre-warmed 0.005% pepsin in 0.01 N HCl solution for 10 min at 37°C. The slides were washed again and then post fixed in 1% paraformaldehyde in PBS for

10 min at RT. To minimize background, RNA was eliminated by incubation in 200 μ g/ml RNase for 30 min in 37°C in a humidified chamber. Finally, the slides were incubated in 2 \times SSC/50% formamide (Sigma-Aldrich) for at least a week before undergoing hybridization.

Generation of the mcb library for chromosome 6

A murine multicolor banding probe set for chromosome 6 was generated as reported in (59). Originally, eight pcp probes were generated by glass needle-based chromosome microdissection (Fig. 1). For the mcb probe set for chromosome 6 (59), the fragments 2, 3, 4, and 5 were used as one pcp probe each. Postmicrodissection, the obtained DNA was amplified by degenerated oligonucleotide-primed PCR (DOP-PCR) as described in (60). The PCR cycles were as follows: a low-stringency program with an initial denaturing step for 10 min at 95°C, four cycles of 1 min at 94°C, 1 min and 30 s at 30°C, and 2 min and 20 s at 72°C. These cycles are followed by a ramp at 72°C (0.2°C/s) and then an extension at 72°C for 3 min. A high-stringency program follows with 34 cycles of 1 min at 94°C, 1 min at 62°C, and 2 min at 72°C (with an increase by 1 s for every cycle). Finally, samples were incubated for an extension at 72°C for 10 min.

Preparation of the probes

The fragment 4 and 7 of chromosome 6 were labeled in a PCR reaction with a degenerate primer DOP in the presence of DIG-11-dUTP (Roche, Basel, Switzerland). The fragment 5 of chromosome 6 was labeled by a DOP-PCR reaction with a degenerate primer and in the presence of biotin-16-dUTP (Roche). The CD8 cosmid was labeled with nick translation (Nick Translation kit, Roche) in the presence of ChromaTide Alexa Fluor 488-5-dUTP (Invitrogen, Carlsbad, CA). After the labeling, all the probes were purified on microspin S200 HR columns (GE Healthcare, Piscataway, NJ) and ethanol precipitated in the presence of mouse cot-1 DNA (Invitrogen) and herring sperm DNA (Sigma-Aldrich).

Hybridization and detection

The slides were taken out of the formamide solution, drained briefly before the hybridization mixture containing the appropriate combination of probes was added, and finally covered with a glass coverslip and sealed with rubber cement. The rubber cement was left to dry completely before denaturation of the slides at 75°C for exactly 4 min. Hybridization was performed for 3 d in a humidified chamber in a 37°C water bath. Three washings were done for 5 min in 2 \times SSC at 37°C, followed by three stringent washings of 5 min in 0.1 \times SSC at 60°C. The slides were then incubated in a 4% BSA in SSC-Tween solution for 10 min at RT. The incubation with the first layer of Abs was carried out in the same solution for 30 min in a humidified chamber in a 37°C water bath, and after extensive washing, the second layer of Abs was applied in the same way. The Abs used in this study were: streptavidin-Alexa Fluor 594 conjugate (Invitrogen), sheep anti-DIG (Roche), and Alexa Fluor 647 donkey anti-sheep IgG (H+L) (Invitrogen), all in a dilution 1:200 in the blocking solution. The final wash was in 2 \times SSC and then DAPI stain was added before mounting them in Vectashield H-1000 (Vector Laboratories, Burlingame, CA) and sealed with a colorless nail polish.

Microscopy and analysis

The slides were examined on an SP2 AOBS or MPSP5 confocal microscope. Images from the confocal were saved as stacks of TIFFs. The pictures were first edited with the Imaris program (Bitplane Scientific Solutions, Zurich, Switzerland). The final measurements were done with StackMeasure, a plugin for ImageJ software (National Institutes of Health, Bethesda, MD). A threshold-based 3D segmentation algorithm to construct surface-based feature models was used, and measurements based on either a center of mass calculation to find the middle or by an exhaustive search through the surface points to find the closest outer edge distance were made. A detailed guide for use of StackMeasure can be found on the following Web site: www.bioinformatics.bbsrc.ac.uk/projects/stackmeasure/.

We excluded from the evaluation all the nuclei that seemed to have been damaged during the experimental procedure.

Chromosome conformation capture

The 3C assay was performed as adapted for the mammalian system (41) with some small modifications. Briefly, 1×10^7 cells were cross-linked in 10 ml DMEM (10% FCS) with 1% formaldehyde for 10 min at room temperature. The cross-linking reaction was quenched by the addition of glycine to a final concentration of 0.125 M. The cells were washed twice in 10 ml 1 \times PBS and were resuspended in 5 ml ice-cold lysis buffer (10 mM Tris [pH 8], 10 mM NaCl, and 0.2% Nonidet P-40) containing protease inhibitors (Roche, 1697498) and incubated on ice for 10 min. Following

centrifugation at 1800 rpm for 5 min at 4°C, the nuclei pellets were frozen via liquid nitrogen and either stored at -80°C for future use or thawed immediately to proceed with the enzyme digestion. Each sample was re-suspended in 0.5 ml of the appropriate 1.2× restriction enzyme buffer (NEB) containing 0.3% SDS and was incubated for 1 h at 37°C while shaking. Triton X-100 was added to 1.8%, and the nuclei were further incubated for 1 h at 37°C to sequester the SDS. Each sample was digested overnight with 800 U restriction enzyme at 37°C while shaking. An additional 400 U enzyme were added the next morning to ensure good digestion efficiency, and the sample was incubated at 37°C for a further 2 h. The reaction was stopped by adding SDS to 1.35% final concentration and incubating at 65°C for 20 min. Cross-links were reversed overnight at 65°C for a quarter of each sample and were used for control Southern blots (Southern, 1975) to check digestion efficiency. They were run on 0.7% agarose gel and hybridized with the probes 0.5RI and CD8α cDNA shown in Supplemental Fig. 3. The remaining sample was diluted into 7 ml 1× ligation buffer (NEB, B0202S) containing 1% Triton X-100 and incubated for 1 h at 37°C. The cross-linked DNA was ligated using 20000 U T4 DNA ligase (NEB) at 16°C for 4 h followed by 30 min at RT. To reverse the cross-links, the samples were incubated overnight at 65°C in 0.2 M NaCl followed by addition of 300 μg proteinase K for a further 2 h. The following day, the samples were incubated for 30 min at 37°C with 300 μg RNase A and then extracted with phenol:chloroform:IAA and ethanol-precipitated.

The restriction enzymes used for the analysis were BglIII and HindIII. The sizes of the BglIII fragments B, C, D, E, F, A, G, and H were 6.5, 14.6, 6, 3.2, 4.8, 5, 6.6, and 8.1 kb, respectively. The sizes of the HindIII fragments H02, H1, H2, H4, H7, H8, H9, and H11 shown in this study were 6.9, 8.8, 2.6, 3.3, 4.1, 5.5, 7.1, and 2.1 kb, respectively. The BAC clones used to generate the control templates were: RP23-139M18 (CHORI) for the CD8 locus and RP24-335G16 (CHORI) for the hprt locus. The BACs were digested (without prior cross-linking) with an excess of restriction enzyme and ligated with T4 DNA ligase at a DNA concentration of 300 ng/μl. The fragments analyzed were 1.5 kb apart for the BglIII digest and 7.4 kb for the HindIII digest. The equal efficiency of enzyme digestion in different BglIII sites (data not shown) as well as the quality of the digestion in the different cell populations (Supplemental Fig. 3) was checked by Southern blot analysis. At least three independent templates were prepared for each cell population and each experiment was repeated at least three times (see also figure legends).

PCR analysis of the ligation products

All the PCR reactions were performed using SYBR green PCR master mix (Applied Biosystems, Foster City, CA). PCR cycles were as follows: an initial denaturing step for 10 min at 95°C; the appropriate number of cycles (typically 38 cycles for the cross-linked, 34 cycles for the control template, and 50 cycles for the real-time method) of 30 s at 94°C, 45 s at 60°C, and 1 min at 72°C; and one final step of 10 min at 72°C. A 7900HT Fast Real-Time machine (Applied Biosystems) was used for the quantitation of the PCR products. The CT values were converted into a fold difference of the amount of each PCR product in relation to the amount at a given point of the reaction, which arbitrarily was given the value of 1. The formula used was $1/2^{CT}$, assuming the PCR amplification efficiency to be 2 for all the primer sets. When quantitation was done from the gel, the PCR reactions were performed using a Dynad Thermal Cycler (Bio-Rad, Hercules, CA), and the products were run on 2% agarose gel without ethidium bromide and quantified using a Storm 850 PhosphoImager and Image Quant 5.0 software (GE Healthcare, Piscataway, NJ). Each PCR reaction was done in duplicate or triplicate, and the data presented in this paper are the average of results for all PCR reactions done. Cross-linking frequencies were calculated using the equation $X_{CD8 \text{ locus}} = [S_{CD8 \text{ locus}}/S_{hprt}]_{\text{cell type}} / [S_{CD8 \text{ locus}}/S_{hprt}]_{\text{BAC}}$.

PCR primers

The primers used for the 3C analysis of the CD8 locus when digested with Bgl II were: 3C-4, 5'-CACAGCAGTGAGGGTGTCAA-3'; 3C-6, 5'-TCTTTC-AGGCCGCTAGTCAG-3'; 3C-7, 5'-ACCTAAGCCAGAACACCTTTG-3'; 3C-8, 5'-GACTCACAAACCACCCATAATG-3'; 3C-9, 5'-CCAATTGG-AAGAGGGCACTAG-3'; 3C-12, 5'-AACTCACAGCAGCTGTAGTTG-3'; 3C-13, 5'-CAGTGGCAGCTGTTTACCA-3'; 3C-14, 5'-GCAGAG-CACTTGGGTTCTTA-3'; 3C-17, 5'-ACCAACTTGGCATGCTAGAGT-3'; 3C-18, 5'-GCATATGCCAAACGGGAGTTG-3'; and 3C-5b, 5'-TAG-CACCTGGAGACTAATG-3'.

For the hprt locus, the primers used were: 3C-25, 5'-CACCATTTCCT-TGACCAGTG-3' and 3C-29, 5'-TAACCTGTGCTGCCTGTGAA-3'.

The primers used for the CD8 locus when digested with HindIII were: H02.2, 5'-CTGTAGTTCTGGTTAGCTGG-3'; H1.3, 5'-AGTTCTGCTG-CTGCCAGATG-3'; H2.4, 5'-AGCCATCTACTCTCTCAGG-3'; H4.2,

5'-GGTTACTGAGATCCTGTCT-3'; H7.3, 5'-GAGTAGGGAATACTG-AGACC-3'; H8.1, 5'-GCAAGAGTGGCTGAAAGAAG-3'; H8.4, 5'-AG-GGCACATGGATCCATACA-3'; H9.3, 5'-CACAGCTTTCTTCTTAGG-C-3'; H11.2, 5'-AGAGTCTAGCTGAGGCTAAG-3'.

For the hprt locus, the primers used were: HB1, 5'-GGCTTAAGGCAA-AACCACTG-3' and HB3, 5'-ACTGGTCAAGGAAATGGTGC-3'.

In the 3D FISH experiments, we made use of a degenerate primer: 5'-CC-GACTCCAAGNNNNNNATGTGG-3'.

Results

Generation of subchromosomal territory probes

To have a more detailed picture of the CD8 gene localization in reference to its chromosomal backbone, a large fragment of the chromosome that bears the CD8 gene (subchromosomal territory [sCT]) was employed as a probe in 3D FISH studies. For the current study, chromosome 6 mcb fragments 4 and 5 containing the CD8α gene locus, both harboring the zone C3 of the chromosome, were used (Fig. 1A). Chromosome 6 mcb fragment 7 containing the CD4 gene was also used (Fig. 1A).

To allow the visualization of its position in the nucleoplasm relative to its chromosomal backbone at different developmental stages, thymocytes from 4–6-wk-old C57BL/6 female mice were sorted in subpopulations: CD4⁻CD8⁻ DN, CD4⁺CD8⁺ DP, CD4⁺CD8⁻ (CD4 SP), and CD4⁻CD8⁺ (CD8 SP) SP thymocytes. mcb fragment 4 and/or fragment 5 was used as a chromosomal backbone reference point and a CD8α cosmid as a probe for the CD8α gene; the nuclear boundaries were identified by staining with DAPI. The slides were examined on an SP2 AOBS or MPSP5 confocal microscope, and image stacks were first analyzed with the Imaris software (Bitplane Scientific Solutions). Fig. 1B–E shows a hybridization

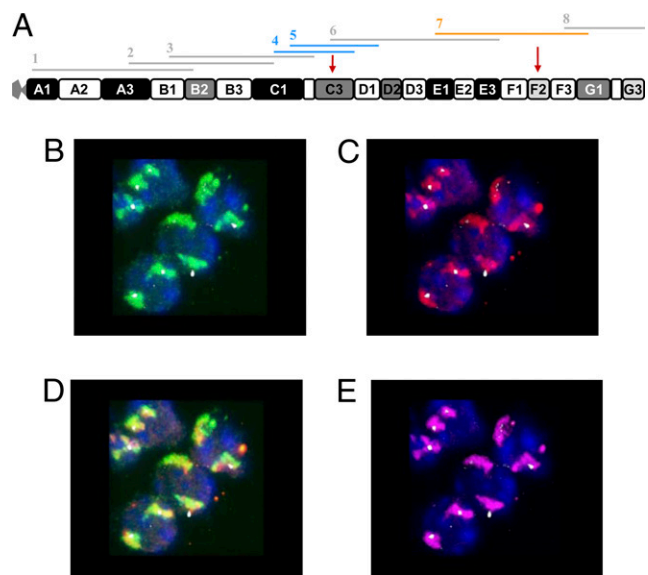


FIGURE 1. A, Making the probes for the sCT. The library of the eight overlapping fragments of the metaphase mouse chromosome 6. CD8α locus is located in the C3 domain of chromosome 6. For the studies of the CD8 repositioning in the nucleus, fragment 4 that harbors domains C1 and C3 or/and fragment 5 that harbors C1 to D1 were used (in blue). For the studies of the CD4 relocalization in the nucleus, fragment 7 that harbors the E1 to G1 domains of chromosome 6 was employed (in orange). B–E, Imaging of the cells on the SP2 and MPSP5 confocal microscope using a 100×/1.4NA objective (Leica Microsystems, Bannockburn, IL). B, Fragment 4 of chromosome 6 was labeled with Alexa 647 (green). In all the images, CD8α was labeled with Alexa 488 (white), and the nucleus was stained with DAPI (blue). C, Fragment 5 of chromosome 6 was labeled with Alexa 594 (red). D, The two chromosomal fragments overlap as expected because they both contain the domains C1 and C3. E, The image stack used in the analysis. The nucleus is in blue, the CD8α locus in white, and the chromosomal overlap (fragments 6.4 and 6.5) in purple.

signal with mcb fragment 4 of chromosome 6 as green (Fig. 1B) and mcb fragment 5 as red (Fig. 1C). The CD8 α cosmid signal is shown as white and the nuclear boundaries as blue (DAPI). Fig. 1D shows the colocalization of the signals from the two chromosomal fragments (in green and red) and allows a colocalization channel to be defined; Fig. 1E shows the overlap of the signals from the two chromosomal mcb fragments as a new channel in purple. Chromosomal backbone is defined either as the overlap of the signals from mcb fragments 4 and 5 (in spleen samples) or as the signal generated from mcb fragment 4 (in thymocytes).

CD8 gene localization in relation to the sCT edge

To assess the position of the CD8 gene relative to its sCT, the distance between the center of the gene hybridization signal and the nearest edge of its chromosome backbone was measured as an absolute value (in micrometers). A value that scores as positive indicates that the gene is outside the sCT, and a negative value indicates that the two entities overlap. Fig. 2A suggests that the CD8 α gene is buried within its sCT in the DN thymocyte population as the average distance from the nearest CT edge has a negative value ($-0.245 \mu\text{m}$). In DP thymocytes, the gene moves away from the sCT to an average distance of $0.28 \mu\text{m}$ from the nearest backbone edge. In CD4 SP thymocytes, the gene retracts closer to the surface of the sCT to an average distance of $0.106 \mu\text{m}$. The distance of the CD8 α locus from its CT in the CD8 SP thymocyte reaches values of $0.383 \mu\text{m}$. Such differences in distance between the center of the gene and the edge of the nearest territory edge could either reflect a fluctuation in the size of the sCT itself or an active movement of the CD8 α gene away from its chromosomal backbone.

CD8 gene loops out from its sCT at different developmental stages in the thymus

To distinguish between the two possibilities mentioned above, the respective volumes of the sCT mcb hybridization signals and the distance between the center of the gene signal and the center of the sCT were measured. mcb hybridization signal values for the sCT indicated alterations in its volume in the different cell types (Fig. 2B). Interestingly, it seems to increase in nonexpressing cells (average value $8.729 \mu\text{m}^3$ in the DN and $8.162 \mu\text{m}^3$ in the CD4 SP cells) and contract in expressing cells (average volume of $5.274 \mu\text{m}^3$ in the DP cells and $6.025 \mu\text{m}^3$ in the CD8 SP).

To relate the CD8 α gene location to an undisputed and immutable point of reference, the distance from the center of the chromosomal backbone signal to the center of the gene signal in the different cell populations was measured. As shown in Fig. 2C, these distances follow the same trend as those between the center of the gene signal to the nearest sCT edge. In CD8 nonexpressing cells (DN and CD4 SP thymocytes) the gene seems to be located much closer to its sCT at an average of 1.118 and $1.039 \mu\text{m}$, respectively. In DP and CD8 SP thymocytes, the distance of the gene from the center of its sCT increases to an average of $1.528 \mu\text{m}$ and $1.508 \mu\text{m}$, respectively. In summary, these data indicate that the CD8 α gene loops out from its sCT during the T cell development in expressing cell types.

CD8 gene nuclear localization in lymphocytes from peripheral lymphoid organs

To examine the positioning of the CD8 gene in the nucleus of mature lymphocytes in peripheral tissues, B cells and CD4 $^+$ and CD8 $^+$ lymphocytes from spleens of C57BL/6 female mice 4 to 6 wk old were sorted to a purity of $\sim 95\%$. In this set of experiments, the chromosomal backbone was represented by the overlap between mcb fragment 4 and mcb fragment 5, giving a better definition of the territory that harbors the CD8 α gene.

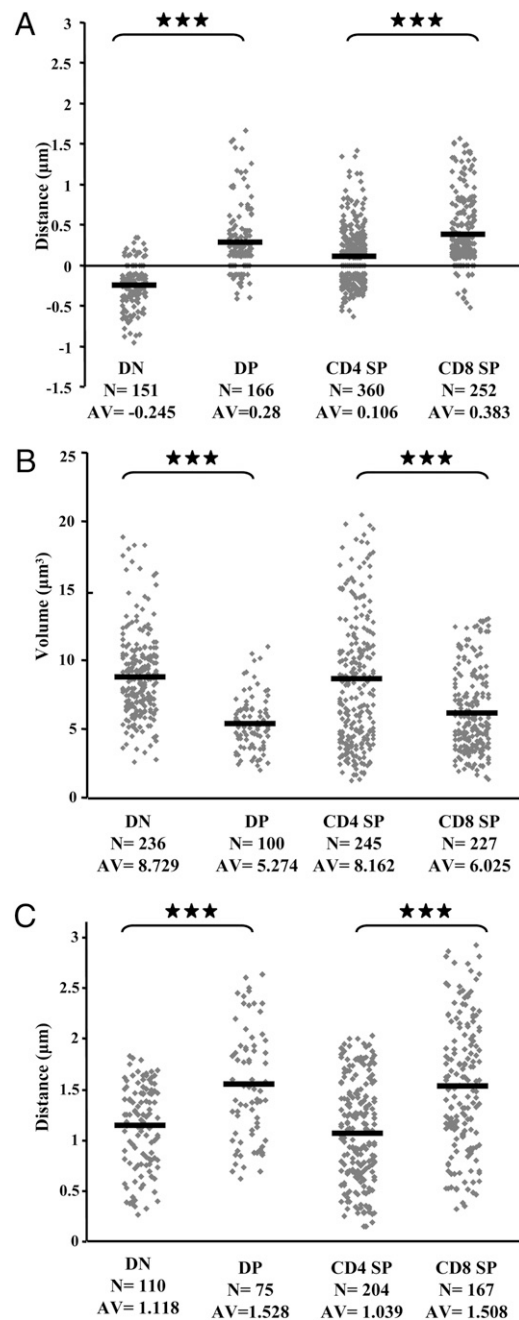


FIGURE 2. The CD8 α repositioning in the nucleus of the thymocytes at different developmental stages. DN, DP, CD4 SP, and CD8 SP thymocytes were isolated from 4–6-wk-old C57BL/6 female mice. In all the graphs, N indicates number of events, and AV indicates average. The distances are measured in micrometers. A Student *t* test was performed for all the comparisons. A, Distances between the center of the CD8 α gene and the nearest edge of its sCT. The negative values indicate that the gene is located inside its sCT and the positive values that it is outside the sCT boundaries. In the DN population, the gene is buried inside its sCT, whereas in the DP cells, it moves away from it ($p = 2.442\text{E-}35$). The differences CD4SP versus CD8SP are significant ($p = 1.9579\text{E-}18$). B, Comparison of the volume of the sCT. In the CD8 nonexpressing cells (DN and CD4 SP), the volume of the chromosomal backbone is considerably bigger than in the expressing cells (DP and CD8 SP). The differences recorded are statistically significant ($p = 6.73142\text{E-}23$ for the DN-DP and $p = 4.99836\text{E-}09$ for the CD4 SP and CD8 SP). C, The distances from the center of the CD8 α to the center of the fragment 4 of chromosome 6 were measured. The differences between DN and DP as well as CD4 SP and CD8 SP are statistically significant ($p = 4.50315\text{E-}08$; $p = 2.96742\text{E-}14$, respectively). ***Statistically significant differences. AV, average; N, number of events.

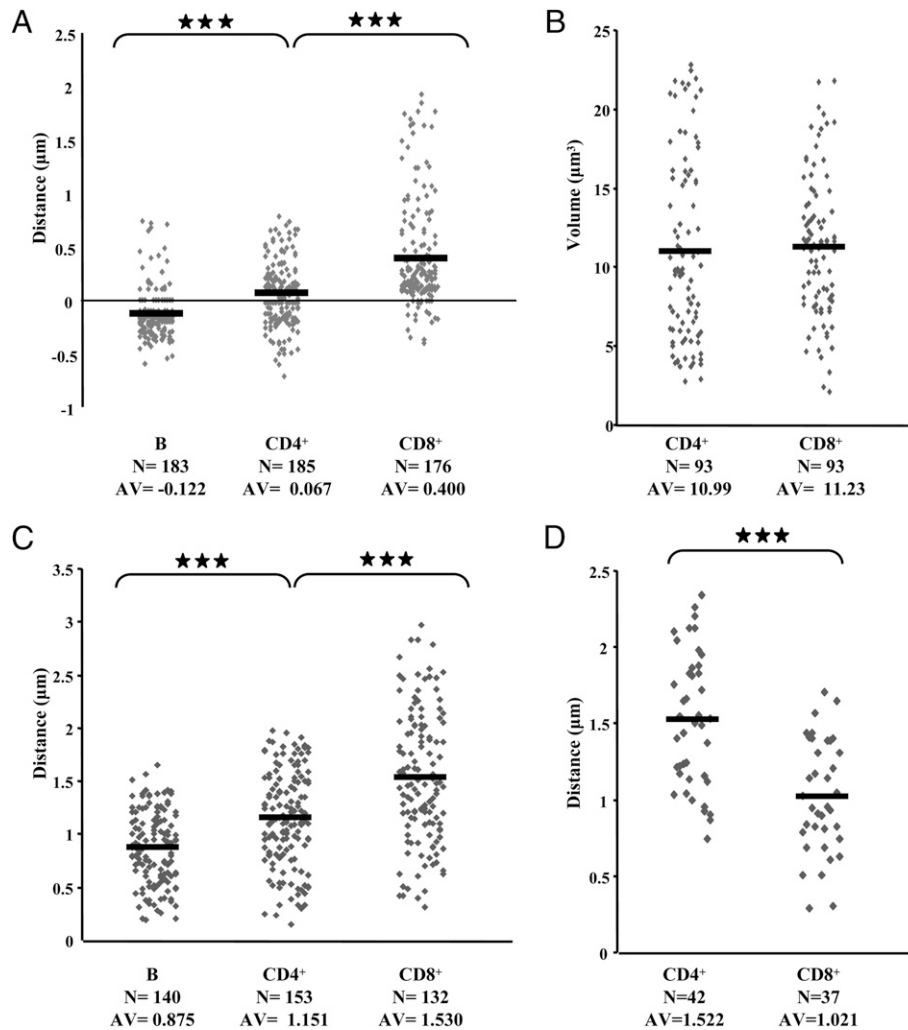


FIGURE 3. The CD8 α and CD4 repositioning in the nucleus of the lymphocytes in the spleen. *B*, CD4⁺CD8⁻ and CD4⁺CD8⁺ lymphocytes were sorted from the spleen of 4–6-wk-old C57BL/6 female mice. The distances are measured in micrometers. *A* Student *t* test was performed for all the comparisons. *A*, Comparison of the distances between the center of the CD8 α gene and the nearest edge of the overlap of the sCT 6.4 and 6.5. The negative values indicate that the gene is buried inside the sCT (in B cells) and the positive values that it extends beyond the sCT (CD4⁺CD8⁻ and CD4⁺CD8⁺ cells). The differences between both B-CD4⁺ and CD4-CD8⁺ comparison are statistically significant: $p = 1.2658E-11$; $p = 5.6484E-14$, respectively. *B*, Comparison of the volume of the sCTs in CD4⁺ and CD8⁺ populations. The relative sizes of the chromosome loci (the overlap between mcb fragment 4 and fragment 5) in the CD4⁺ and CD8⁺ populations were measured, and no significant differences were observed (0.754935). *C*, The distances between the center of the CD8 locus to the center of the overlap between the chromosomal fragments 6.4 and 6.5 were measured. All the differences are significant ($p = 8.48599E-09$ for the B-CD4 comparison and $p = 6.36905E-09$ for the CD4-CD8 comparison). *D*, The relative distance between the center of CD4 gene and the center of the chromosome fragment 6.7 (shown in Fig. 1C) was measured. This difference is statistically significant ($p = 5.93692E-07$). ***Statistically significant differences. AV, average; N, number of events.

Fig. 3A shows that in B cells, the CD8 α gene has an average distance from the nearest edge of its territory of $-0.122 \mu\text{m}$, suggesting that the gene is within the sCT boundaries. In the CD4⁺ cells, the CD8 α gene is also close to the surface of the sCT with an average distance of $0.067 \mu\text{m}$. In the cells that express CD8, the gene is clearly located outside the sCT at an average distance of $0.400 \mu\text{m}$. To rule out the possibility that the changes we observed in the distances between the gene and the edge of the corresponding territory are due to the fluctuations of the size of the territories in the different cell populations, the volume of the territory in different cells was determined. Fig. 3B shows a plot of the measurements of the volumes of the 4 and 5 chromosome 6 mcb fragments overlap in CD4⁺ and CD8⁺ cells. The values $10.99 \mu\text{m}^3$ and $11.23 \mu\text{m}^3$, for the CD4⁺ and the CD8⁺ cells, respectively, are very similar, with no statistically significant difference between the two populations. The findings suggest that in the peripheral lymphoid tissues, the volume of the

sCT harboring the CD8 gene remains the same in the different cell types.

To corroborate the above findings, the mean distance between the center of CD8 α gene to the center of the overlap of the signal from the two mcb probes was measured in the three populations. Fig. 3C shows that in B lymphocytes, the CD8 α gene seems to be very close to the center of the chromosomal backbone, with an average distance of $0.875 \mu\text{m}$. In the mature CD4⁺ and CD8⁺ population, the differential position of the gene in relation to its sCT reflects the one observed in the CD4 SP and CD8 SP thymocytes, at $1.151 \mu\text{m}$ and $1.530 \mu\text{m}$, respectively.

CD4 gene localization in different lymphocyte populations

To study how the CD4 gene behaves in the CD4⁺ and CD8⁺ cells in the periphery, a cosmid that contains the CD4 gene was employed as a probe, and mcb fragment 7 of the chromosome 6 library that harbors the CD4 gene was used as a probe for its sCT. In Fig. 3D, the

distances between the centers of the CD4 gene and mbc fragment 7 fluorescent signals were measured. Interestingly, the CD4 gene remains closer to the center of the chromosomal backbone in the CD8⁺ cells (1.021 μm) and extends further away in the CD4 expressing cells (1.522 μm). Thus, the CD4 gene seems to move away from its territory in CD4-expressing cells, whereas in CD8⁺ cells, it is retracted closer to its sCT.

Taken together, our data demonstrate unequivocally that gene expression in lymphocytes is accompanied by the relocation of the locus outside its sCT. Our data are in agreement with previous studies showing that the expression of a gene can be accompanied by its nuclear repositioning in relation to its sCT, possibly to reach out to TFs.

3C analysis along the CD8 locus in total thymocytes

To identify possible 3D interactions between regulatory elements in the CD8 locus that could be temporally related to its repositioning as described in the previous sections, the 3C technique (31) was used, as modified for the mammalian system (41) and in which the cross-linking frequency of two restriction fragments, as measured by the amount of a ligation product, is proportional to the frequency with which these two genomic fragments interact.

The organization of the CD8α and CD8β gene loci and the fragments used for the 3C analysis are shown in Fig. 4A. Initially, the interactions of BglIII fragments B (CIV-1, 2, 3), C (CIV-4, 5, 6), D (CIII-1, 2), E (CIII-3), F (CII-1, 2), G (control), and H (CI-1, 2, 3), covering different regulatory elements of the CD8 locus, with fragment A (promoter of the CD8α gene), were checked. The murine hprt housekeeping gene expressed in all the cell types was used as a control.

The 3C template was prepared from total thymocytes, which consist of 80–90% of cells expressing the CD8α and CD8β genes (DP and CD8 SP) from C57BL/6 mice. A real-time PCR method was used, as described in *Materials and Methods*, and the average relative cross-linking frequencies are shown in Fig. 4B. Notably, all the relative cross-linking frequencies were found to be very similar to each other, with no significant peaks of interactions, and

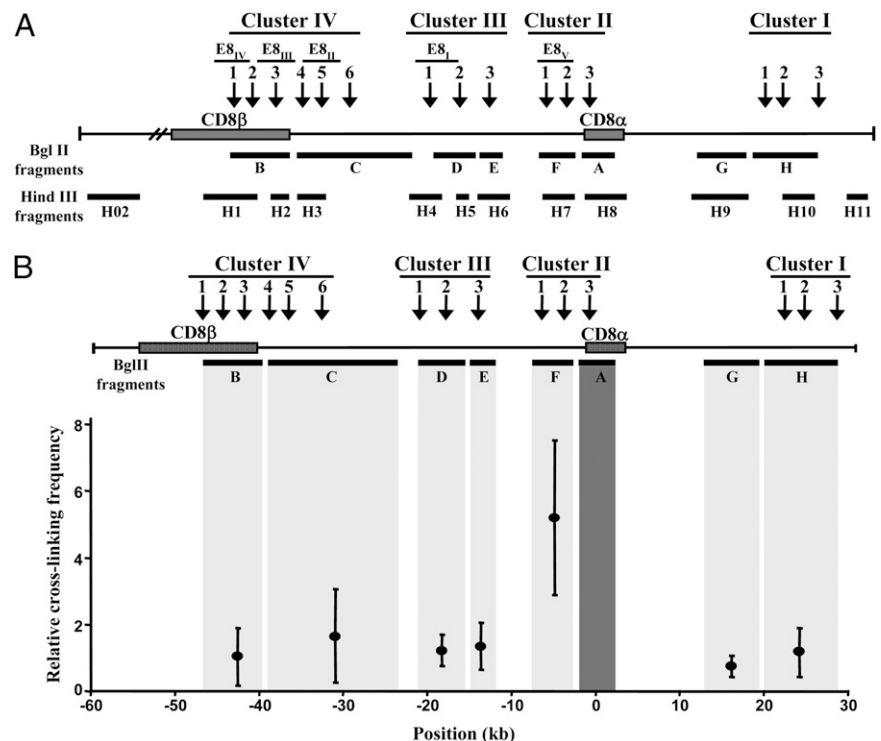
low, but above the value of 1, which is considered to reflect the background in these experiments. The only exception was control fragment G, which does not contain any known regulatory element related to CD8α expression and whose cross-linking frequency was found to be below 0.7. The cross-linking frequency between fragments F-A had the highest value (5.2) as expected, because these fragments are next to each other in the genomic DNA. Interactions between the above fragments and fragment F (CII-1, 2) were also assessed, but again, no significant difference in cross-linking frequencies was observed (data not shown).

Hence, we conclude that in CD8-expressing thymocytes, there are no preferential interactions between any of the previously described regulatory elements and the promoter of the CD8α gene within an 80-kb region of the CD8α and CD8β gene loci. This finding does not exclude the possibility that all these regulatory elements are closer together in CD8-expressing cells compared with nonexpressing cells.

Genes and cis-regulatory elements of the mouse CD8 gene complex cluster spatially in CD8-expressing cells

To compare the spatial organization of the mouse CD8 locus in cells in which the CD8α and CD8β genes are expressed (CD8⁺) with cells in which they are silenced (CD4⁺) or have never been transcribed (B cells), lymphocytes from spleens of wild-type C57BL/6 mice were sorted, and 3C analysis was performed. It is important to note that the CD4⁺ and CD8⁺ cell populations isolated from the spleen are not homogeneous, as they also contain cells that are CD44^{high}. However, the great majority of them (~90%) are CD44^{low} (data not shown). Fig. 5A shows the relative cross-linking frequencies of fragments B (CIV-1, -2, -3), D (CIII-1, -2), and G (control) with fragment A (CD8α promoter) in the three populations, as measured by real-time PCR. To be able to show many experiments in the same graph, the value of cross-linking frequency of each fragment pair in CD8-expressing cells was set to 100%, and the rest of the values were expressed as a percentage of that in each experiment. This analysis showed a great reduction in the cross-

FIGURE 4. 3C analysis in the mouse CD8 locus in total thymocytes. *A*, Schematic presentation of the mouse CD8 gene locus showing the location of the CD8α and CD8β genes (filled boxes). Vertical arrows indicate the individual DNase I hypersensitive sites. Horizontal bars indicate the restriction fragments used for the 3C analysis and are labeled A–H for the BglIII digest and H02–H11 for the HindIII digest. *B*, Relative cross-linking frequencies along the CD8 locus observed in total thymocytes. In all of the graphs, light gray shaded vertical bars indicate the position and size of the analyzed fragments, and the dark gray shaded bar represents the fixed fragment. Four different 3C templates were prepared, and the relative cross-linking frequency of each fragment pair shown is the average of at least five independent experiments. The x-axis shows the relative position in the locus. Error bars represent SEM. All the cross-linking frequencies were measured by real-time PCR.



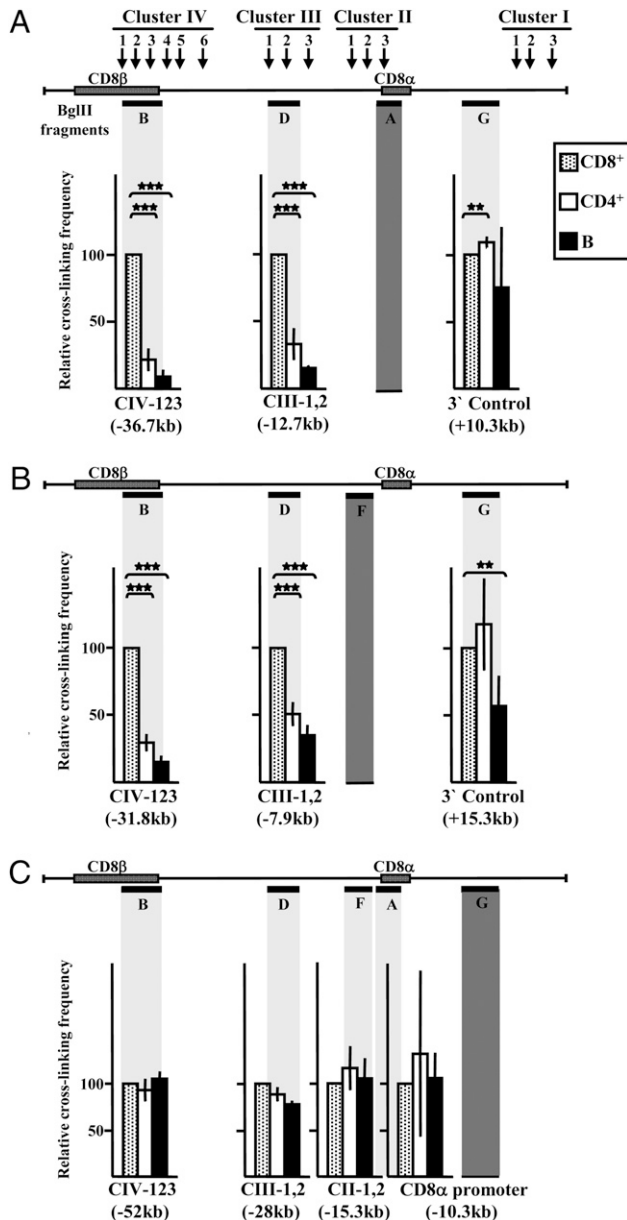


FIGURE 5. *Cis*-regulatory elements of the mouse CD8 locus, as well as the CD8 α and CD8 β genes, spatially cluster in CD8-expressing cells. The organization of the mouse CD8 gene locus and the BglIII restriction fragments are shown. Sorted CD8⁺, CD4⁺, and B cells from spleens of C57BL/6 mice were used to prepare 3C templates. Three independent templates were prepared for each cell population. The experiment was repeated three times for the CD4⁺ cells and four times for the CD8⁺ and B cell template. The gray (CD8⁺ cells), white (CD4⁺ cells), and black (B cells) bars shown in the graphs are average values. The relative position in the CD8 locus of each fragment analyzed is shown underneath the graphs (point 0 is the fixed fragment every time). Error bars represent SEM. All cross-linking frequencies were measured by real-time PCR. Cross-linking frequencies shown are not corrected for PCR amplification efficiency; therefore, only signals obtained with the same primer set can be compared. *A*, Crosslinking frequencies of fragments B (CIV-1, 2, 3), D (CIII-1, 2), and G (control) with A (CD8 α promoter). *B*, Cross-linking frequencies of fragments B, D, and G with F (CII-1, 2). *C*, Cross-linking frequencies of fragments B, D, F, and A with G. ** p < 0.01; *** p < 0.001.

linking frequencies of fragments B and D with fragment A in CD4⁺ and B cells compared with CD8⁺ cells. In contrast, cross-linking of fragment G, which does not contain any known regulatory element, to the promoter fragment did not show a statistically significant cross-linking frequency difference between CD8⁺ and B cells.

These results were corroborated by data obtained with a semi-quantitative method (Supplemental Fig. 1). It should be noted that the actual value of the cross-linking frequency in CD8-expressing (CD8⁺ cells) and nonexpressing cells (B cells) for fragments B versus A dropped from 1.4 in CD8⁺ cells to 0.5 in B cells and from 1.6 to 0.8 for D versus A, suggesting an average reduction of 64% and 50%, respectively, in the cross-linking frequencies in B cells compared with CD8⁺ cells. In contrast, there was no difference between the cross-linking frequencies in either population of fragment G with A, which were found to be below the value of 1, indicating low frequency of interaction of this fragment with the promoter of the CD8 α gene (Supplemental Fig. 2).

3C analysis of the locus was also performed using fragment F (CII-1, -2) as the fixed point. Cross-linking frequencies between fragments B, D, and G with fragment F are shown in Fig. 5*B*. Similarly to our previous observation, there was a great decrease in the cross-linking frequencies to fragment F in CD4⁺ and B cells compared with CD8⁺ cells for CIV-1, -2, -3 (fragment B) and CIII-1, -2 (fragment D), indicating a closer proximity in space of these regulatory elements in CD8-expressing cells compared with cells that have silenced the locus. The control fragment (G versus F) in this case showed a big variation between different experiments and cannot be evaluated.

To confirm that fragment G indeed shows no difference between the three populations tested, it was used as the fixed point and interactions with fragments B, D, F, and A were assessed (Fig. 5*C*). This analysis showed that for the majority of the fragment pairs, there was no significant difference between expressing and non-expressing cells, indicating that the distance in space of fragment G with the different regulatory elements of the CD8 locus is the same in CD8⁺, CD4⁺, and B cells.

To corroborate the results obtained with the BglIII digest, the experiment was repeated using HindIII restriction enzyme to generate fragments. The HindIII digest has the additional advantage that gives in general smaller fragments compared with BglIII, something that is thought to reduce the background in the 3C experiments. Fig. 6 shows the results obtained with fragments H1 (CIV-1, -2), H2 (CIV-3), H4 (CIII-1), H7 (CII-1, -2), and H9 (control), using fragment H8 (CD8 α promoter) as the fixed point. In addition to fragment H9 (the equivalent to fragment G in the BglIII digest), fragments H02 (5' control) and H11 (3' control) were also used in this analysis. In this case, the following sorted populations from C57BL/6 wild-type mice were used: DP cells from thymus, CD8⁺, CD4⁺, and B cells from spleen. The 3C templates were prepared and titrated, and the PCR products were measured from the gel. In this case, the values obtained from the DP population for each reaction are set to 100%, and the rest of the values are expressed as a percentage of that in each experiment. In agreement with the BglIII results, we observed a significant decrease in the cross-linking frequencies of fragments H1, H2, and H4 with the promoter of the CD8 α gene in CD4⁺ and B cells compared with DP and CD8⁺ cells. In contrast, all the control fragments (H02, H9, and H11), which do not carry any known elements involved in the regulation of expression of the CD8 α and CD8 β genes, showed the same cross-linking frequencies in all the cell populations. Fragment H7 also showed equal cross-linking frequency in the different populations, as expected, because H7 is located directly next to the fixed fragment H8.

We conclude that the regulatory elements lying within the 40-kb region that contains CIV and CIII are closer in space with the CD8 α gene promoter in cells in which the locus is transcribed and are forming an ACH. Regions of the locus located 5' of CIV (H02) and 3' of the CD8 α gene (H8) do not participate in this ACH. In cells that have silenced (CD4⁺ cells) or have never activated the locus (B cells), the interactions are much weaker, indicating a more linear, nonstructured chromatin conformation in these cells.

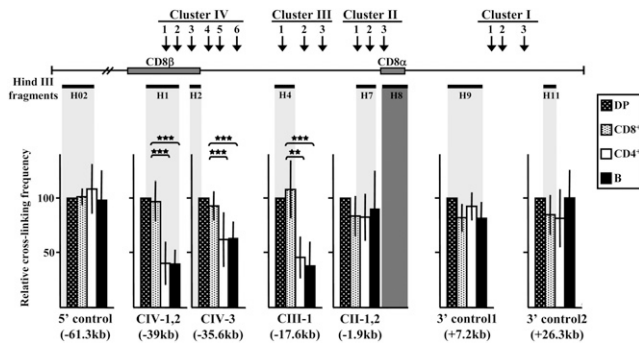


FIGURE 6. *Cis*-regulatory elements within CIV and CIII of the mouse CD8 locus and the CD8 α and CD8 β genes come close together in CD8-expressing cells. The organization of the mouse CD8 gene locus and the HindIII restriction fragments are shown. Sorted DP cells from thymus and CD8⁺, CD4⁺, and B cells from spleens of C57BL/6 mice were used to prepare 3C templates. Four independent templates were prepared for each cell population. The experiment was repeated 9 times for the CD8⁺ and CD4⁺ cells and 12 times for the DP and B cell template. The dark gray (DP cells), light gray (CD8⁺ cells), white (CD4⁺ cells), and black (B cells) bars shown in the graph are average values. Error bars represent SEM. All cross-linking frequencies were measured from the gel. Cross-linking frequencies shown are not corrected for PCR amplification efficiency; therefore, only signals obtained with the same primer set can be compared. ***p* < 0.01; ****p* < 0.001.

Discussion

The functional architecture of the interphase nucleus has recently become a focus of interest. Chromatin modifications and nuclear spatial organization seem to function in concert to coordinate the responses of a cell to environmental and intracellular signals that lead to the establishment of a gene expression program. The positioning of a gene in relation to its CT has been studied by several groups in recent years. It is generally accepted that the genome has distinct R (gene-rich) bands and G (gene-poor) bands and that the RIDGES (regions of increased gene expression) tend to occupy the nuclear center. Gene-dense regions located at the periphery of their CTs are thought to have more chances of associating with a TF as opposed to genes buried in the interior of their territory. Such an arrangement does not exclude genes located within the CT from being transcribed, as TFs have also been found inside the CTs. In some cases, genes that reside in loops that extend from the chromosome core colocalize with focal increased concentrations of RNAPol II, an observation that suggests that they could loop out to reach a TF (61). Looping out, however, cannot be considered as a prerequisite for gene expression (27, 62–65).

In our study, we followed the physical behavior of the CD8 α gene during the developmental program of T cells, from DN thymocytes to DP and then CD4 SP and CD8 SP in the thymus and eventually to mature CD4⁺ and CD8⁺ cells in the spleen, and compared it to B cells. The CD8 gene is located on mouse chromosome 6, and its repositioning was studied in relation to its subchromosomal territory defined by mcb fragments 4 and 5.

When the distance between the center of the gene locus and the nearest edge of the territory was measured, it became apparent that the CD8 α gene was positioned away from its sCT in the thymus, exclusively in expressing cells, namely the DP and CD8 SP thymocytes. In marked contrast, the gene was found close to its sCT in the nonexpressing DN and CD4 SP cells. Two possible configurations could account for this observation: either the size of the sCT fluctuates between the different cell types or the gene relocates away from the sCT by a looping out mechanism. To distinguish between these two possibilities, the volume of the sCT as well as the

distance between the center of the gene to the center of the sCT were estimated. Indeed, the volume of the sCT fluctuated within the thymocyte developmental stages. The molecular basis of these differences remains unclear at the moment. They may reflect differences in the size of the whole nucleus or breathing rearrangement of the territory around the area that harbors the CD8 α locus when the potential loop is generated. However, this finding does not alter the conclusions, as the differences in distance between the center and the gene to the edge of the sCT were corroborated by measurements of the distance between the centers of the two entities. Similar studies were carried out in cells from peripheral lymphoid tissues. It is evident from our data that even though these cells have very similar sizes of chromosome 6 sCT, the CD8 α gene is located differentially from the edge of its sCT in the different cells, probably by a looping out mechanism. In particular, B cells that have never expressed the CD8 α gene seem to have the locus buried in its sCT, whereas in the CD4⁺ population, the CD8 gene is located at the edge of the sCT and loops further away from the center of the sCT in the CD8-expressing cells. Similarly, the CD4 gene is re-located away from its sCT in the expressing cells (CD4⁺) and stays closer to its center in the CD8⁺ population. The observation that two different gene markers of lymphocyte development (CD4 and CD8 genes) move away from their sCT when expressed points to a rather general phenomenon during T cell development that could be explained by the need of the specific transcribing genes to loop out to reach transcription factories present in limited numbers in cell nuclei. In support of our data, other studies have come to the conclusion that gene loci undergoing active transcription often extend from their CT by creating loops with a radius of several microns (25, 26, 66–68). Previously published data indicated that CD4 and CD8 genes are embedded in the total CT, whether they were expressed or not (69). The reason our data appear to contrast this finding probably resides in the fact that in our study, the chromosomal backbone representing the sCT is a more narrowly defined entity, because it is a relatively small part of chromosome 6 that contains either the CD8 α or the CD4 gene, allowing us to have a more accurate view of the gene repositioning upon differentiation.

Gene repositioning could involve an active and directed movement of the gene toward a TF, possibly involving sliding on the nuclear matrix, or alternatively its association with a TF could be a stochastic event. RNA polymerase can provide the driving force, as it has been shown that it generates a pulling power comparable or even higher than this produced by mechanoenzymes (70). The exact mechanism that controls such spatial rearrangements and gene repositioning within the nucleoplasm has yet to be revealed. It is still an open question whether it is the gene moving to pre-existing TFs or whether TFs assemble *de novo* on activated genes. A reconciliation of the accumulating contradictory data regarding the order of events could be that TFs might be generated *de novo* by highly active genes with strong regulatory elements (promoters, enhancers, and LCRs). Upon formation of such TFs, more genes, possibly less active, could get recruited (71). To this end, it is well established that regulatory regions, such as LCRs, can contribute to the relocalization of a gene to the surface of its sCT or even in a loop that brings it away from its sCT, possibly acting as a nucleation point for more genes to share a specific TF (21). It would be interesting to examine the effect on the location of a lymphocyte subset-specific gene, such as the CD8, when it is associated with a pan-lymphocyte-specific regulatory element, such as the hCD2 LCR.

The formation of chromatin loops has been shown to involve direct interactions among distant regulatory elements, such as LCRs, enhancers, and promoters (reviewed in Refs. 72 and 73). Direct *in vivo* evidence to support the looping model has come from studies in the β -globin locus (38, 39, 41), which employ the 3C technique (31). The

clustering of regulatory elements and genes has been called the ACH (41). Subsequently, the existence of long-range interactions has been shown in other gene loci (36, 37, 40, 42). Differential chromatin looping has been reported to regulate CD4 expression in developing thymocytes (74). There have been reports that other elements and protein factors, such as EKLF, CTCF, and GATA-1, are essential to stabilize the long-range interactions (28–30). Our data are consistent with an interpretation that the *cis*-regulatory elements of the CD8 α and CD8 β genes spatially cluster together in CD8-expressing cells, in which the locus is active, to form an ACH. Such close interaction among the different regulatory elements might provide an explanation for the redundancy of regulatory functions observed in regulatory element deletion and transgenic mice (54, 55, 57). It should be noted that this spatial clustering of regulatory elements in the CD8 locus also brings the CD8 β gene in close proximity to the CD8 α gene. The CD8 molecule is expressed as a $\alpha\beta$ heterodimer in all the populations analyzed in this report. Close interaction of the regulatory elements of the two genes could aid their coordinately regulated expression in these cell populations.

DNA sequences ~20 kb downstream of the CD8 α gene are not thought to be involved in CD8 gene regulation and fragments before (G and H9) and after (H11) CI (Fig. 5) were used as control fragments for the 3C experiments. No difference in the cross-linking frequencies between the different populations was observed using these fragments. In addition, the average cross-linking frequency of fragments G–A was found to be lower than B–A, C–A, D–A, and E–A, although the linear distance between fragments G and A is smaller than the distance of fragment A from B, C, D, and E. These findings indicate that the length of the DNA sequences that take part in the CD8 locus ACH is ~40 kb. It should be noted that the 3C technique uses large populations of cells, and therefore the data presented in this study represent average values of a bulk population and cannot provide the dynamics of chromatin reorganization on a per-cell basis.

A poised conformation of transcription complexes has been proposed for promoters and other regulatory elements before actual transcription starts. It is speculated that the ACH takes shape first, creating the appropriate environment to recruit the transcriptional machinery. In the case of the Th2 locus, the existence of a preformed configuration has been suggested in which other factors are also required for the stabilization of the structure (40). The mouse β -globin LCR also acquires such a conformation, interacting with other DNase I hypersensitive sites in the locus, in erythroid progenitors that do not yet express the β -globin genes (38, 39). Notably, a difference in the spatial conformation among nonexpressing brain cells, erythroid progenitors (poised state), and differentiated erythrocytes (expressing cells) is clearly shown. Interestingly, our data presented in this paper show that in B cells that have never activated the CD8 locus, the interaction frequencies of the CD8 regulatory elements were lower than in CD4⁺ cells that have expressed the CD8 molecule at some point in their development. This suggests that although both these cell types do not express the CD8 α and CD8 β genes, the past transcriptional history of the locus is reflected in its present 3D chromatin conformation. This is supported by the finding that the CD8 gene is closer or embedded within its sCT when compared with its location in CD4⁺ cells, in which it is found nearer the surface of the sCT.

Taken together, our results suggest that during T cell development, the CD8 gene in CD8-expressing cells relocates from an inner core of its chromosomal domain to a nuclear location where transcription becomes possible. As this is also true for the CD4 gene, this gene motility appears to be a more general feature of gene regulation during T cell development. This relocation appears to be temporally associated with a clustering of regulatory elements forming a tight ACH. In contrast, in nonexpressing cells, the gene remains within or close to the main body of its chromosomal domain, and the regulatory elements of the locus appear not to

interact with each other. These observations confirm the dynamic state of chromatin during developmental state decisions.

Acknowledgments

We thank the members of the Divisions of Molecular Immunology and Immune Cell Biology at the National Institute for Medical Research for helpful discussions; in particular, Dr. Nikolai Belyaev, Dr. Alexander Savelev, and Dr. Henrique Veiga-Fernandes as well as Michelle Burke for excellent secretarial assistance. We also thank all the members of the sorting and animal facilities and the Confocal Image Analysis Laboratory.

Disclosures

The authors have no financial conflicts of interest.

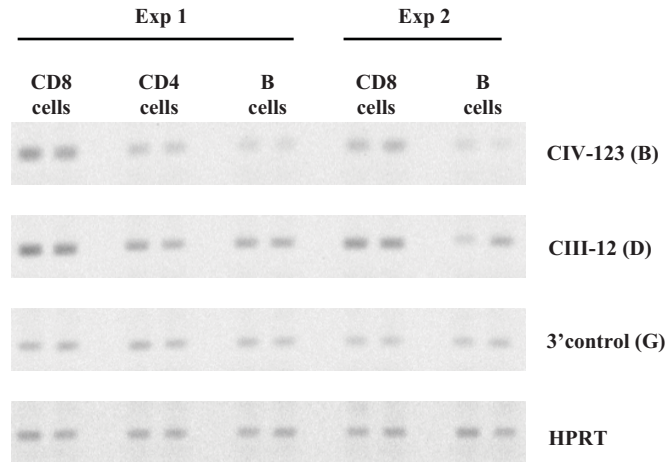
References

1. Iourov, I. Y., T. Liehr, S. G. Vorsanova, and Y. B. Yurov. 2007. Interphase chromosome-specific multicolor banding (ICS-MCB): a new tool for analysis of interphase chromosomes in their integrity. *Biomol. Eng.* 24: 415–417.
2. Manvelyan, M., F. Hunstig, S. Bhatt, K. Mrasek, F. Pellestor, A. Weise, I. Simonyan, R. Aroutiounian, and T. Liehr. 2008. Chromosome distribution in human sperm – a 3D multicolor banding-study. *Mol. Cytogenet.* 1: 25.
3. Manvelyan, M., F. Hunstig, K. Mrasek, S. Bhatt, F. Pellestor, A. Weise, and T. Liehr. 2008. Position of chromosomes 18, 19, 21 and 22 in 3D-preserved interphase nuclei of human and gorilla and white hand gibbon. *Mol. Cytogenet.* 1: 9.
4. Manvelyan, M., P. Kempf, A. Weise, K. Mrasek, A. Heller, A. Lier, K. Höffken, H. J. Fricke, H. G. Sayer, T. Liehr, and H. Mkrtchyan. 2009. Preferred colocalization of chromosome 8 and 21 in myeloid bone marrow cells detected by three dimensional molecular cytogenetics. *Int. J. Mol. Med.* 24: 335–341.
5. Brown, K. E., J. Baxter, D. Graf, M. Merkenschlager, and A. G. Fisher. 1999. Dynamic repositioning of genes in the nucleus of lymphocytes preparing for cell division. *Mol. Cell* 3: 207–217.
6. Delaire, S., Y. H. Huang, S. W. Chan, and E. A. Robey. 2004. Dynamic repositioning of CD4 and CD8 genes during T cell development. *J. Exp. Med.* 200: 1427–1435.
7. Merkenschlager, M., S. Amoils, E. Roldan, A. Rahemtulla, E. O'connor, A. G. Fisher, and K. E. Brown. 2004. Centromeric repositioning of coreceptor loci predicts their stable silencing and the CD4/CD8 lineage choice. *J. Exp. Med.* 200: 1437–1444.
8. Jackson, D. A., A. B. Hassan, R. J. Errington, and P. R. Cook. 1993. Visualization of focal sites of transcription within human nuclei. *EMBO J.* 12: 1059–1065.
9. Lemke, J., J. Claussen, S. Michel, I. Chudoba, P. Mühlig, M. Westermann, K. Sperling, N. Rubtsov, U. W. Grummt, P. Ullmann, et al. 2002. The DNA-based structure of human chromosome 5 in interphase. *Am. J. Hum. Genet.* 71: 1051–1059.
10. Weise, A., H. Starke, A. Heller, C. Uwe, and T. Liehr. 2002. Evidence for interphase DNA decondensation transverse to the chromosome axis: a multicolor banding analysis. *Int. J. Mol. Med.* 9: 359–361.
11. Amrichová, J., E. Lukášová, S. Kozubek, and M. Kozubek. 2003. Nuclear and territorial topography of chromosome telomeres in human lymphocytes. *Exp. Cell Res.* 289: 11–26.
12. Goetze, S., J. Mateos-Langerak, H. J. Gierman, W. de Leeuw, O. Giromus, M. H. Indemans, J. Koster, V. Ondrej, R. Versteeg, and R. van Driel. 2007. The three-dimensional structure of human interphase chromosomes is related to the transcriptome map. *Mol. Cell. Biol.* 27: 4475–4487.
13. Küpper, K., A. Kölbl, D. Biener, S. Dittrich, J. von Hase, T. Thormeyer, H. Fiegler, N. P. Carter, M. R. Speicher, T. Cremer, and M. Cremer. 2007. Radial chromatin positioning is shaped by local gene density, not by gene expression. *Chromosoma* 116: 285–306.
14. Neusser, M., V. Schubel, A. Koch, T. Cremer, and S. Müller. 2007. Evolutionarily conserved, cell type and species-specific higher order chromatin arrangements in interphase nuclei of primates. *Chromosoma* 116: 307–320.
15. Sadoni, N., S. Langer, C. Fauth, G. Bernardi, T. Cremer, B. M. Turner, and D. Zink. 1999. Nuclear organization of mammalian genomes. Polar chromosome territories build up functionally distinct higher order compartments. *J. Cell Biol.* 146: 1211–1226.
16. Federico, C., C. D. Cantarella, C. Scavo, S. Saccone, B. Bed'Hom, and G. Bernardi. 2005. Avian genomes: different karyotypes but a similar distribution of the GC-richest chromosome regions at interphase. *Chromosome Res.* 13: 785–793.
17. Federico, C., S. Saccone, L. Andreozzi, S. Motta, V. Russo, N. Carels, and G. Bernardi. 2004. The pig genome: compositional analysis and identification of the gene-richest regions in chromosomes and nuclei. *Gene* 343: 245–251.
18. Saccone, S., C. Federico, and G. Bernardi. 2002. Localization of the gene-richest and the gene-poorest isochores in the interphase nuclei of mammals and birds. *Gene* 300: 169–178.
19. Francastel, C., M. C. Walters, M. Groudine, and D. I. Martin. 1999. A functional enhancer suppresses silencing of a transgene and prevents its localization close to centromeric heterochromatin. *Cell* 99: 259–269.
20. Noordermeer, D., M. R. Branco, E. Splinter, P. Klous, W. van Ijcken, S. Swagemakers, M. Koutsourakis, P. van der Spek, A. Pombo, and W. de Laat. 2008. Transcription and chromatin organization of a housekeeping gene cluster containing an integrated beta-globin locus control region. *PLoS Genet.* 4: e1000016.

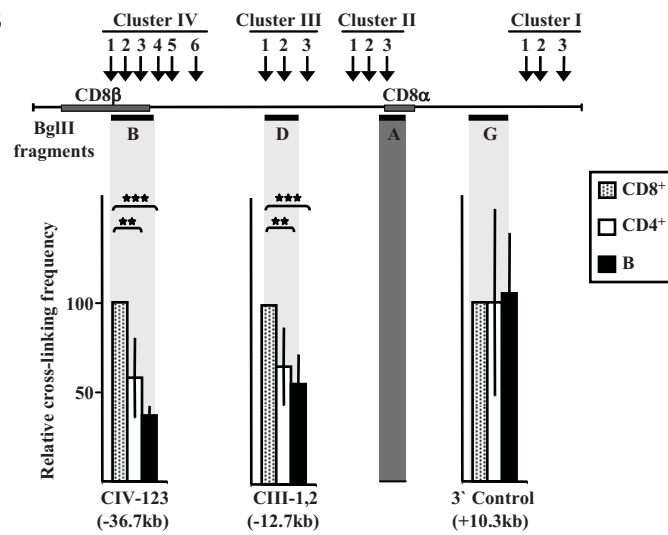
21. Ragozy, T., A. Telling, T. Sawado, M. Groudine, and S. T. Kosak. 2003. A genetic analysis of chromosome territory looping: diverse roles for distal regulatory elements. *Chromosome Res.* 11: 513–525.
22. Bártová, E., and S. Kozubek. 2006. Nuclear architecture in the light of gene expression and cell differentiation studies. *Biol. Cell* 98: 323–336.
23. Lanctôt, C., C. Kaspar, and T. Cremer. 2007. Positioning of the mouse Hox gene clusters in the nuclei of developing embryos and differentiating embryoid bodies. *Exp. Cell Res.* 313: 1449–1459.
24. Gandhi, M. S., J. R. Stringer, M. N. Nikiforova, M. Medvedovic, and Y. E. Nikiforov. 2009. Gene position within chromosome territories correlates with their involvement in distinct rearrangement types in thyroid cancer cells. *Genes Chromosomes Cancer* 48: 222–228.
25. Mahy, N. L., P. E. Perry, and W. A. Bickmore. 2002. Gene density and transcription influence the localization of chromatin outside of chromosome territories detectable by FISH. *J. Cell Biol.* 159: 753–763.
26. Volpi, E. V., E. Chevret, T. Jones, R. Vatcheva, J. Williamson, S. Beck, R. D. Campbell, M. Goldsworthy, S. H. Powis, J. Ragoussis, et al. 2000. Large-scale chromatin organization of the major histocompatibility complex and other regions of human chromosome 6 and its response to interferon in interphase nuclei. *J. Cell Sci.* 113: 1565–1576.
27. Mahy, N. L., P. E. Perry, S. Gilchrist, R. A. Baldock, and W. A. Bickmore. 2002. Spatial organization of active and inactive genes and noncoding DNA within chromosome territories. *J. Cell Biol.* 157: 579–589.
28. Drissen, R., R. J. Palstra, N. Gillemans, E. Splinter, F. Grosveld, S. Philipsen, and W. de Laat. 2004. The active spatial organization of the beta-globin locus requires the transcription factor EKLF. *Genes Dev.* 18: 2485–2490.
29. Splinter, E., H. Heath, J. Kooren, R. J. Palstra, P. Klous, F. Grosveld, N. Galjart, and W. de Laat. 2006. CTCF mediates long-range chromatin looping and local histone modification in the beta-globin locus. *Genes Dev.* 20: 2349–2354.
30. Vakoc, C. R., D. L. Letting, N. Gheldof, T. Sawado, M. A. Bender, M. Groudine, M. J. Weiss, J. Dekker, and G. A. Blobel. 2005. Proximity among distant regulatory elements at the beta-globin locus requires GATA-1 and FOG-1. *Mol. Cell* 17: 453–462.
31. Dekker, J., K. Rippe, M. Dekker, and N. Kleckner. 2002. Capturing chromosome conformation. *Science* 295: 1306–1311.
32. Dostie, J., T. A. Richmond, R. A. Arnaout, R. R. Selzer, W. L. Lee, T. A. Honan, E. D. Rubio, A. Krumm, J. Lamb, C. Nusbaum, et al. 2006. Chromosome Conformation Capture Carbon Copy (5C): a massively parallel solution for mapping interactions between genomic elements. *Genome Res.* 16: 1299–1309.
33. Simonis, M., P. Klous, E. Splinter, Y. Moshkin, R. Willemsen, E. de Wit, B. van Steensel, and W. de Laat. 2006. Nuclear organization of active and inactive chromatin domains uncovered by chromosome conformation capture-on-chip (4C). *Nat. Genet.* 38: 1348–1354.
34. Simonis, M., J. Kooren, and W. de Laat. 2007. An evaluation of 3C-based methods to capture DNA interactions. *Nat. Methods* 4: 895–901.
35. Zhao, Z., G. Tavoosidana, M. Sjölander, A. Göndör, P. Mariano, S. Wang, C. Kanduri, M. Lezcano, K. S. Sandhu, U. Singh, et al. 2006. Circular chromosome conformation capture (4C) uncovers extensive networks of epigenetically regulated intra- and interchromosomal interactions. *Nat. Genet.* 38: 1341–1347.
36. Liu, Z., and W. T. Garrard. 2005. Long-range interactions between three transcriptional enhancers, active *Vkappa* gene promoters, and a 3' boundary sequence spanning 46 kilobases. *Mol. Cell Biol.* 25: 3220–3231.
37. Murrell, A., S. Heeson, and W. Reik. 2004. Interaction between differentially methylated regions partitions the imprinted genes *Igf2* and *H19* into parent-specific chromatin loops. *Nat. Genet.* 36: 889–893.
38. Palstra, R. J., B. Tolhuis, E. Splinter, R. Nijmeijer, F. Grosveld, and W. de Laat. 2003. The beta-globin nuclear compartment in development and erythroid differentiation. *Nat. Genet.* 35: 190–194.
39. Patrinos, G. P., M. de Krom, E. de Boer, A. Langeveld, A. M. Imam, J. Strouboulis, W. de Laat, and F. G. Grosveld. 2004. Multiple interactions between regulatory regions are required to stabilize an active chromatin hub. *Genes Dev.* 18: 1495–1509.
40. Spilianakis, C. G., and R. A. Flavell. 2004. Long-range intrachromosomal interactions in the T helper type 2 cytokine locus. *Nat. Immunol.* 5: 1017–1027.
41. Tolhuis, B., R. J. Palstra, E. Splinter, F. Grosveld, and W. de Laat. 2002. Looping and interaction between hypersensitive sites in the active beta-globin locus. *Mol. Cell* 10: 1453–1465.
42. Vermimmen, D., M. De Gobbi, J. A. Sloane-Stanley, W. G. Wood, and D. R. Higgs. 2007. Long-range chromosomal interactions regulate the timing of the transition between poised and active gene expression. *EMBO J.* 26: 2041–2051.
43. Lomvardas, S., G. Barnea, D. J. Pisapia, M. Mendelsohn, J. Kirkland, and R. Axel. 2006. Interchromosomal interactions and olfactory receptor choice. *Cell* 126: 403–413.
44. Spilianakis, C. G., M. D. Lalioti, T. Town, G. R. Lee, and R. A. Flavell. 2005. Interchromosomal associations between alternatively expressed loci. *Nature* 435: 637–645.
45. Fowlkes, B. J., and D. M. Pardoll. 1989. Molecular and cellular events of T cell development. *Adv. Immunol.* 44: 207–264.
46. Kioussis, D., and W. Ellmeier. 2002. Chromatin and CD4, CD8A and CD8B gene expression during thymic differentiation. *Nat. Rev. Immunol.* 2: 909–919.
47. Jay, G., M. A. Palladino, G. Khoury, and L. J. Old. 1982. Mouse Lyt-2 antigen: evidence for two heterodimers with a common subunit. *Proc. Natl. Acad. Sci. USA* 79: 2654–2657.
48. Ledbetter, J. A., and W. E. Seaman. 1982. The Lyt-2, Lyt-3 macromolecules: structural and functional studies. *Immunol. Rev.* 68: 197–218.
49. Ledbetter, J. A., W. E. Seaman, T. T. Tsu, and L. A. Herzenberg. 1981. Lyt-2 and lyt-3 antigens are on two different polypeptide subunits linked by disulfide bonds. Relationship of subunits to T cell cytolytic activity. *J. Exp. Med.* 153: 1503–1516.
50. Lefrancois, L. 1991. Phenotypic complexity of intraepithelial lymphocytes of the small intestine. *J. Immunol.* 147: 1746–1751.
51. Gorman, S. D., Y. H. Sun, R. Zamoyska, and J. R. Parnes. 1988. Molecular linkage of the Ly-3 and Ly-2 genes. Requirement of Ly-2 for Ly-3 surface expression. *J. Immunol.* 140: 3646–3653.
52. Hostert, A., M. Tolaini, R. Festenstein, L. McNeill, B. Malissen, O. Williams, R. Zamoyska, and D. Kioussis. 1997. A CD8 genomic fragment that directs subset-specific expression of CD8 in transgenic mice. *J. Immunol.* 158: 4270–4281.
53. Ellmeier, W., M. J. Sunshine, K. Losos, F. Hatam, and D. R. Littman. 1997. An enhancer that directs lineage-specific expression of CD8 in positively selected thymocytes and mature T cells. *Immunity* 7: 537–547.
54. Ellmeier, W., M. J. Sunshine, K. Losos, and D. R. Littman. 1998. Multiple developmental stage-specific enhancers regulate CD8 expression in developing thymocytes and in thymus-independent T cells. *Immunity* 9: 485–496.
55. Ellmeier, W., M. J. Sunshine, R. Maschek, and D. R. Littman. 2002. Combined deletion of CD8 locus cis-regulatory elements affects initiation but not maintenance of CD8 expression. *Immunity* 16: 623–634.
56. Garefalaki, A., M. Coles, S. Hirschberg, G. Mavria, T. Norton, A. Hostert, and D. Kioussis. 2002. Variegated expression of CD8 alpha resulting from in situ deletion of regulatory sequences. *Immunity* 16: 635–647.
57. Hostert, A., A. Garefalaki, G. Mavria, M. Tolaini, K. Roderick, T. Norton, P. J. Mee, V. L. Tybulewicz, M. Coles, and D. Kioussis. 1998. Hierarchical interactions of control elements determine CD8alpha gene expression in subsets of thymocytes and peripheral T cells. *Immunity* 9: 497–508.
58. Hostert, A., M. Tolaini, K. Roderick, N. Harker, T. Norton, and D. Kioussis. 1997. A region in the CD8 gene locus that directs expression to the mature CD8 T cell subset in transgenic mice. *Immunity* 7: 525–536.
59. Trifonov, V., C. Karst, U. Claussen, K. Mrasek, S. Michel, P. Avner, and T. Liehr. 2005. Microdissection-derived murine mcb probes from somatic cell hybrids. *J. Histochem. Cytochem.* 53: 791–792.
60. Liehr, T., A. Heller, H. Starke, N. Rubtsov, V. Trifonov, K. Mrasek, A. Weise, A. Kuechler, and U. Claussen. 2002. Microdissection based high resolution molecular banding for all 24 human chromosomes. *Int. J. Mol. Med.* 9: 335–339.
61. Osborne, C. S., L. Chakalova, K. E. Brown, D. Carter, A. Horton, E. Debrand, B. Goyenechea, J. A. Mitchell, S. Lopes, W. Reik, and P. Fraser. 2004. Active genes dynamically colocalize to shared sites of ongoing transcription. *Nat. Genet.* 36: 1065–1071.
62. Abranches, R., A. F. Beven, L. Aragón-Alcaide, and P. J. Shaw. 1998. Transcription sites are not correlated with chromosome territories in wheat nuclei. *J. Cell Biol.* 143: 5–12.
63. Morey, C., N. R. Da Silva, P. Perry, and W. A. Bickmore. 2007. Nuclear reorganization and chromatin decondensation are conserved, but distinct, mechanisms linked to Hox gene activation. *Development* 134: 909–919.
64. Sadoni, N., and D. Zink. 2004. Nascent RNA synthesis in the context of chromatin architecture. *Chromosome Res.* 12: 439–451.
65. Verschure, P. J., I. van Der Kraan, E. M. Manders, and R. van Driel. 1999. Spatial relationship between transcription sites and chromosome territories. *J. Cell Biol.* 147: 13–24.
66. Brown, J. M., J. Leach, J. E. Reittie, A. Atzberger, J. Lee-Prudhoe, W. G. Wood, D. R. Higgs, F. J. Iborra, and V. J. Buckle. 2006. Coregulated human globin genes are frequently in spatial proximity when active. *J. Cell Biol.* 172: 177–187.
67. Chambeyron, S., and W. A. Bickmore. 2004. Chromatin decondensation and nuclear reorganization of the HoxB locus upon induction of transcription. *Genes Dev.* 18: 1119–1130.
68. Williams, R. R., S. Broad, D. Sheer, and J. Ragoussis. 2002. Subchromosomal positioning of the epidermal differentiation complex (EDC) in keratinocyte and lymphoblast interphase nuclei. *Exp. Cell Res.* 272: 163–175.
69. Kim, S. H., P. G. McQueen, M. K. Lichtman, E. M. Shevach, L. A. Parada, and T. Misteli. 2004. Spatial genome organization during T-cell differentiation. *Cytogenet. Genome Res.* 105: 292–301.
70. Yin, H., M. D. Wang, K. Svoboda, R. Landick, S. M. Block, and J. Gelles. 1995. Transcription against an applied force. *Science* 270: 1653–1657.
71. Sutherland, H., and W. A. Bickmore. 2009. Transcription factories: gene expression in unions? *Nat. Rev. Genet.* 10: 457–466.
72. Dekker, J. 2008. Gene regulation in the third dimension. *Science* 319: 1793–1794.
73. Palstra, R. J., M. Simonis, P. Klous, E. Brassat, B. Eijkelkamp, and W. de Laat. 2008. Maintenance of long-range DNA interactions after inhibition of ongoing RNA polymerase II transcription. *PLoS One* 3: e1661.
74. Jiang, H., and B. M. Peterlin. 2008. Differential chromatin looping regulates CD4 expression in immature thymocytes. *Mol. Cell Biol.* 28: 907–912.

Ktistaki_Supplementary figure1

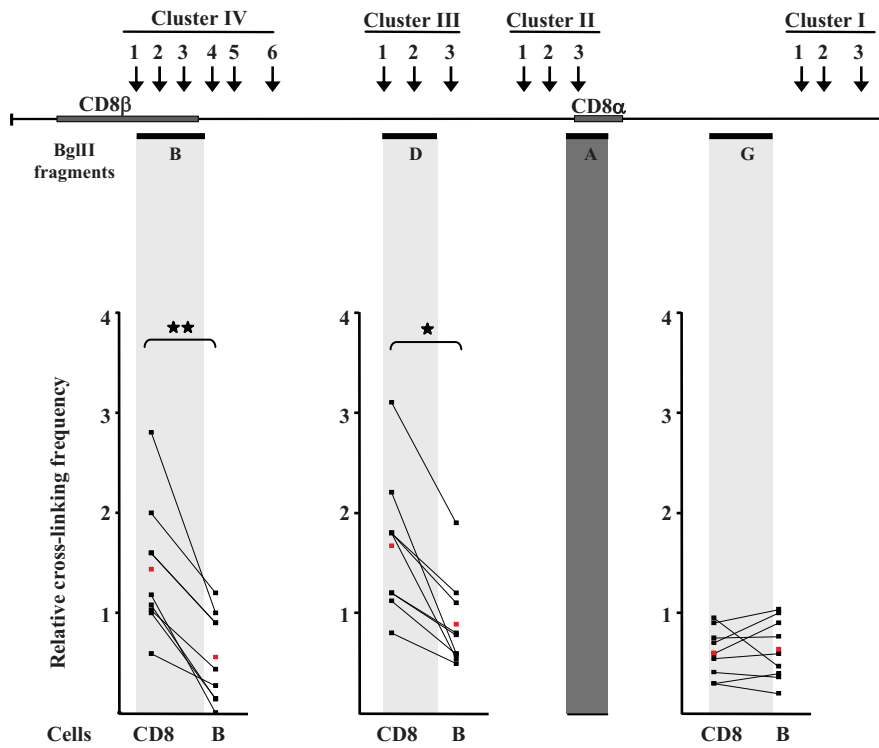
A



B

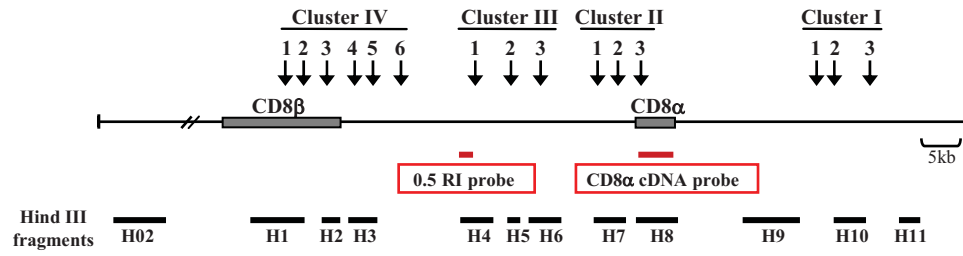


Ktistaki_Supplementary figure 2

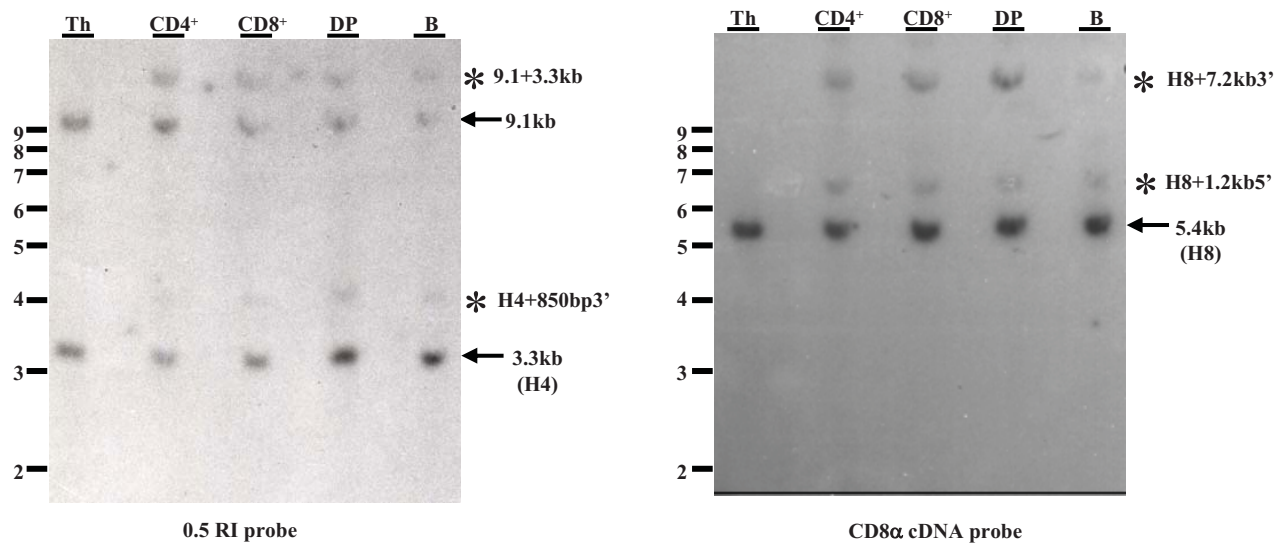


Ktistaki_Supplementary figure 3

A



B



Supplementary figure 1. *Cis*-regulatory elements of the mouse CD8 locus, as well as the CD8 α and CD8 β genes, spatially cluster in CD8 expressing cells. **A**, An example of PCR-amplified ligation products on 2% agarose gel without ethidium bromide. Two independent CD8 and B cell templates are shown and one CD4 template. Each reaction was done in duplicate in this case. The fragments where the PCR primers are located are shown on the right. The PCR products of the control locus *hprt* are also shown. **B**, The organisation of the mouse CD8 gene locus and the Bgl II restriction fragments are shown. Sorted CD8⁺, CD4⁺ and B cells from spleen of C57Bl/6 mice were used to prepare 3C templates. Three independent templates were prepared for the CD4⁺ cells and four templates for the CD8⁺ and B cell population. The experiment was repeated 3 times for the CD4⁺ cells and 9 times for the CD8⁺ and B cell template. The grey (CD8⁺ cells), white (CD4⁺ cells) and black (B cells) bars shown in the graphs are average values. Error bars represent s.e.m. (***) P<0.001, ** P<0.01). All crosslinking frequencies were measured from the gel. Crosslinking frequencies shown are not corrected for PCR amplification efficiency; therefore, only signals obtained with the same primer set can be compared. Crosslinking frequencies of fragments B (CIV-1,2,3), D (CIII-1,2) and G (control) with A (CD8 α promoter) are shown.

Supplementary figure 2. Reduced interactions of *cis*-regulatory elements in the CD8 locus and the CD8 α gene in B cells compared to CD8 cells. The organisation of the mouse CD8 gene locus and the Bgl II restriction fragments labelled B, C, D, E, F, A, G and H are shown. The actual crosslinking frequencies measured from 9 independent experiments are shown in the graphs. The values in CD8⁺ and B cells obtained from the same experiment are linked. The red dot represents the average value in each case. (** P<0.01, * P<0.05).

Supplementary figure 3. Digestion efficiency of crosslinked chromatin is the same in different cell populations. **A**, The organisation of the mouse CD8 gene locus and the Hind III restriction fragments are shown. Red horizontal bars show the probes (0.5 RI probe and CD8 α cDNA probe) used for the hybridisation. **B**, Southern blot hybridisation using the probes 0.5 RI (left) and CD8 α cDNA (right). The cell population is shown on top. Arrows indicate the parental bands recognised by the probe in each case. Asterisks indicate partial digests. Horizontal bars on the left of each blot indicate sizes of DNA molecules in kilobases. Crosslinked CD4⁺, CD8⁺, DP and B cell templates were digested with Hind III. In order to check the efficiency of the digestion, 25% of each template (digested, but not ligated) was then used for Southern blot hybridisation. The same blot was successively hybridised with the two probes and is shown here. The thymus (Th) sample was digested without prior crosslinking and represents complete digestion.